Variable temperature infrared spectroscopy: A convenient tool for studying the thermodynamics of weak solid–gas interactions

Edoardo Garrone*[a] and Carlos Otero Areán*[b]

Received 11th May 2005
First published as an Advance Article on the web 23rd August 2005
DOI: 10.1039/b407049f

This *tutorial review* describes the use of variable temperature infrared spectroscopy of adsorbed species (VTIR), a recent method for studying the thermodynamics of weak solid–gas interactions. Examples show how a fundamental relationship of thermodynamics (the van't Hoff equation, used long since in several fields of physical chemistry) can describe equilibrium processes at the solid–gas interface. The VTIR method is fully exploited by measuring absorbance of an IR band, temperature and pressure over a wide temperature range: an estimation of the interaction energy is, however, possible even ignoring the equilibrium pressure. Precise thermodynamic characterization of solid–gas interactions is required in several fields: on the applied side, gas sensing, separation and storage, which involve such areas as work-place security, air pollution control and the energy sector; regarding fundamental knowledge, weak solid–gas interactions are relevant to a number of fields, including hydrogen bonding, coordination chemistry and surface phenomena in a broad sense.

Infrared (IR) spectroscopy of (gas) molecules adsorbed on a solid is frequently used to characterize both, the adsorbed species and the adsorbing centres at the solid surface. The potential of the technique can be greatly enhanced by obtaining IR spectra over a temperature range, and simultaneously measuring IR absorbance, temperature and equilibrium pressure. When this is done, variable temperature infrared (VTIR) spectroscopy can be used not only for a more detailed surface characterization, but also for precise studies on the thermodynamics of solid–gas interactions. Furthermore, when weak interactions are concerned, the technique shows favourable features compared to adsorption calorimetry, or to other classical methods. The potential of the VTIR method is highlighted by reviewing recently reported studies on dihydrogen, dinitrogen and carbon monoxide adsorption on zeolites. To facilitate understanding, an outline of the basis of the method is also given, together with an appraisal of the critical points involved in its practical use.

1 Introduction

The search for porous solids having improved gas adsorption properties constitutes a forefront issue of current technological development, triggered by strategic, industrial and environmental needs. Porous adsorbents can be used, *inter alia*, for gas sensing, separation and storage. Gas sensing finds widespread application in many areas, including the workplace and the domestic environment. Gas separation (using porous solids) is currently used in pressure-swing adsorption processes, which are applied, for instance, for oxygen separation from air and for hydrogen separation from a variety of feedstocks; such as refinery off-gas and hydrogen rich gas from steam reforming of hydrocarbons. On the other hand, the development of suitable, cost-effective, adsorbents for large scale (reversible) gas storage and transport is a present-day strategic issue in the energy sector, propelled mainly by the potential use of hydrogen as an energy vector in a sustainable (and cleaner) energy scenario.

For most of the foregoing processes, weak solid–gas interactions are highly significant, and means for studying

[a]*Dipartimento di Scienza dei Materiali ed Ingegneria Chimica, Politecnico di Torino, 10129 Turin, Italy. E-mail: edoardo.garrone@polito.it; Fax: +39 0115644699*
[b]*Departamento de Química, Universidad de las Islas Baleares, 07122 Palma de Mallorca, Spain. E-mail: dqueep0@uib.es*

Edoardo Garrone

Edoardo Garrone graduated in Chemistry in 1966, becoming a full professor in 1994. He was first at the University of Turin (Italy) and he is currently at the Polytechnic University of the same town. His interests have always been in the field of surface processes, covering different aspects from physisorption to chemical reactivity by means of methods as different as quantum mechanics, classical spectroscopies (IR, UV-Vis, EPR) and thermodynamics. The systems most studied have been pure oxides of catalytic interest, zeolites and mesoporous silica-aluminas.

them, both at the mechanistic and the thermodynamic level, are needed. Weak solid–gas interactions give rise to (reversible) physisorption, and involve mainly van der Waals type forces; frequently of the ion-dipole, ion-quadrupole and ion-induced dipole type. The energy balance involved is usually in the range of 2 to 20 kJ mol^{-1}, hence posing demanding requirements on its experimental measurement.

Classically, experimental determination of the energy involved in gas–solid interaction relies on three techniques. Adsorption calorimetry, temperature programmed desorption (TPD), and evaluation of isosteric heats of adsorption. In the first case, the heat evolved during gas adsorption is directly measured. Excellent reviews exist[1,2] on the subject, relating the experimentally measured adsorption heat to thermodynamically defined parameters, and considering the possible experimental set-ups, *e.g.* closed or open systems. The essence of adsorption calorimetry can be summarised as follows. Let q be the total heat evolved when N moles of a gas are adsorbed. If the adsorbing system has ideal features, *i.e.* exhibits sites which are all equal and non interacting (Langmuir model), the molar heat evolved Q/N coincides with the differential heat of adsorption, $q = \partial Q/\partial N$, and both of them are constant. In the vast majority of cases, however, $Q/N \neq \partial Q/\partial N$, and the differential heat of adsorption (the quantity more usually considered) is observed to decrease with coverage, θ. In short, $q = q(\theta)$, with $\partial q/\partial\theta < 0$. The intricacies of any non-ideal system (presence of different adsorbing sites, heterogeneity among structurally equivalent sites, or interaction among sites) are all reflected in the function $q = q(\theta)$.

The second way to extract information about adsorption energy is to study the release of adsorbed molecules as a function of a rising temperature of the adsorbent–adsorbate system, kept under a dynamic vacuum; this is the basis of the TPD method. The pressure measured in a TPD run is basically a measure of the gas desorption rate: a qualitative interpretation is straightforward, relating the number of desorption peaks observed to different types of adsorbing sites in the solid adsorbent. For the same adsorbed molecule, the temperature at which the TPD signal peaks gives an indication on the strength of the gas–solid interaction. A more sophisticated analysis makes use of different temperature sweep rates, and facilitates access to the activation energy for desorption; when the adsorption stage is (as often happens) non activated, this coincides with the adsorption energy. Also on this widely used technique comprehensive reviews are available.[3]

The function $q = q(\theta)$ can, in principle, be obtained through the third main procedure referred to above; the evaluation of isosteric heats of adsorption. Here, a set of adsorption isotherms measured at different temperatures is considered, and the quantity $-RT^2\partial\ln p/\partial T$ is evaluated at constant θ, p being the equilibrium pressure ensuring the given coverage at the temperature T. This quantity differs from $q = q(\theta)$ by a mere RT term.

Calorimetry and TPD are applicable to all types of adsorption processes, whereas the isosteric heat method applies only to reversible adsorption. When weak interactions are considered, all three methods are in principle applicable. The main point, however, is that the temperature at which the adsorption experiment can be run has necessarily to be low. This concept can be further developed by considering the equilibrium between a gaseous and an adsorbed phase at their standard states: equilibrium implies that variation of Gibbs free energy, ΔG, is nil. On the other hand, for a process involving standard states, $\Delta G = \Delta G^\circ$, and therefore $\Delta G^\circ = \Delta H^\circ - T^*\Delta S^\circ = 0$. Hence, T^*, the actual temperature of the experimental measurement, is given by $\Delta H^\circ/\Delta S^\circ$. In many instances, for any given adsorbed gas, ΔS° is roughly considered to be constant, because of the prevailing role of the loss of translational degrees of freedom. More refined considerations lead to a functional dependence between ΔH° and ΔS°: an example will be given below (Section 5). Under the approximation of constant ΔS°, ΔH° is seen to scale approximately with T^*. Hence, experimental study of weak interactions (*i.e.*, those involving small ΔH° values) necessarily requires low temperature measurements. Low temperature calorimetry is a well developed technique, but it is cumbersome and expensive to operate. Basically, the same holds for low-temperature TPD. The measurement of gas adsorption isotherms at a low temperature, usually around the boiling point of nitrogen, is instead a common procedure. The drawback is (as stated above) that the isosteric heat of adsorption is an all-encompassing quantity, the detailed interpretation of which requires the quantitative information on energy to be coupled with qualitative information on the nature of the adsorbing sites; such as (for instance) that coming from IR spectroscopic measurements. It is relevant to note that isosteric heats and their dependence upon coverage may be computed *via* the intensity of specific IR bands of adsorbed species, as done by several authors.[4–7]

On the computational side (not reviewed here), presently developing at a brisk pace, there are several approaches to calculate gas–solid interaction energies. Weak interactions, however, where the contribution of dispersive (London type) interactions is important, are not easy to account for by any of the computational approaches presently available. This is particularly true for light molecules like dihydrogen.

Carlos Otero Areán

Carlos Otero Areán was educated at the University of Madrid (Complutense) and obtained PhD degrees in Chemistry from the Universities of Bath (UK) and Madrid. He has carried out postdoctoral research at the French CNRS (Orléans) and at the University of Oxford (ICL). Currently, he is Professor of Inorganic Chemistry at the Universidad de las Islas Baleares (Spain), where his main research interests are in several aspects of solid state and surface chemistry, including the interaction between inorganic solids and biological molecules.

On the side of the experimental approach, it has been recently shown[8] that, in favourable cases, IR spectroscopy of adsorbed species at a variable temperature (VTIR) can yield accurate values of both the standard enthalpy of adsorption, ΔH°, and the corresponding change in entropy, ΔS°, even when dealing with very weak interactions. Note that a necessary condition for the VTIR method to be applied is that the adsorption process brings about a characteristic IR absorption band in the adsorbed molecule or a specific change in a characteristic IR absorption band of the adsorbing centre. However, when at least one of these requirements is met with, the VTIR method has the potential to, (*i*) discriminate between different adsorption sites which might be present in the same adsorbent, and (*ii*) give site-specific thermodynamic data (under favourable circumstances). These are further (and important) advantages over classical adsorption calorimetry, which add to the fact that VTIR spectroscopy can be experimentally less demanding than low-temperature calorimetry. The VTIR method has been used for studying many (weakly interacting) gas–solid systems. Among them, those selected for reviewing (mainly with a view to enlighten the potential of the method) include dihydrogen, dinitrogen and carbon monoxide adsorbed on several protonic and cation-exchanged zeolites, which frequently show a single type of (isolated) adsorption site; so that Langmuir type adsorption prevails. Among the surface processes examined are: (*i*) formation of 1 : 1 surface adducts (*e.g.*, with dihydrogen or carbon monoxide); (*ii*) transformation of 1 : 1 into 1 : 2 adducts (*e.g.* monocarbonyl into dicarbonyl species); (*iii*) carbonyl–isocarbonyl isomerization processes; and (*iv*) hydrogen-bonding to surface Brønsted acid sites. Examples will follow. However, with a view to facilitate understanding for the non-specialised reader, relevant details of the VTIR spectroscopic method for studying weak solid–gas interactions will first be analysed.

2 Basis of the VTIR method

The VTIR method is based on the use of the van't Hoff equation relating the change in any equilibrium to precisely ΔH° and ΔS°. The general form of this equation reads:

$$[\partial \ln K/\partial T]_p = \Delta H^\circ/RT^2 \qquad (2.1)$$

where K is the equilibrium constant of the process being considered. If the usual assumption is made that both ΔH° and ΔS° are temperature independent, the van't Hoff relationship becomes:

$$\ln K(T) = (-\Delta H^\circ/RT) + (\Delta S^\circ/R) \qquad (2.2)$$

The central idea of the VITR method is that K can be determined from precise knowledge of the intensity of a characteristic IR absorption band (assumed to be proportional to the coverage of the relevant adsorbed species) and the corresponding equilibrium pressure. Despite its standard use in other fields of physical chemistry, the van't Hoff equation has very seldom been applied to studies of gas–solid interactions. Experimentally, this approach involves the use of an IR cell which allows IR spectra to be recorded over a wide temperature range while simultaneously measuring temperature and equilibrium pressure. Some commercial cells are adaptable for such a purpose; however, most of the experimental results discussed below were obtained by using a home made cell described in detail elsewhere.[9] Measurements are run by dosing a fixed amount of the adsorbate gas into the cell which contains the solid adsorbent wafer, after which the cell is closed and VTIR spectra are taken (at an increasing temperature) without altering the total amount of adsorbate. However, because of the variable temperature, partition of the adsorbate between the gas and the adsorbed phase changes. It should be noted that a variable temperature infrared cell (used as described above) constitutes a closed system in the thermodynamic sense, in contrast to calorimetric or volumetric adsorption measurements which are usually performed in open systems. Since the whole series of spectra is recorded while keeping the cell closed, pressure increases with increasing temperature; and the rising pressure partially counteracts desorption brought about when temperature is raised. The temperature range over which adsorption can be observed is thus enlarged, which constitutes an advantage when dealing with weak solid–gas interactions.

Referring to adsorption on a single type of surface site, with formation of 1 : 1 adducts, the VTIR method can be summarised as follows. Let S be the empty surface site, and M the adsorbed molecule. The adsorption process can be described by the eqn (2.3) below:

$$S_{(s)} + M_{(g)} \rightleftarrows S\text{–}M_{(ads)} \qquad (2.3)$$

For an ideal system, the activity of the occupied sites is given by the coverage, θ, and that of the empty sites by $1 - \theta$, while the activity of molecules in the gas phase is given by the corresponding equilibrium pressure, p. This leads to the Langmuir equation (2.4) below:

$$\theta = N/N_M = K(T)p/[1 + K(T)p] \qquad (2.4)$$

where N is the number of adsorbed moles under a pressure p, and N_M that at full coverage. Other assumptions are: (*i*) validity of the van't Hoff integrated equation (2.2), and (*ii*) validity of the Lambert–Beer law; which states that the intensity, A, of the characteristic IR absorption band is proportional to the amount adsorbed,

$$A = bN \text{ (}b\text{, being a proportionality constant).} \qquad (2.5)$$

Consequently, full coverage corresponds to the maximum intensity, A_M, of the IR absorption band. Combination of the eqn (2.2), (2.4), and (2.5) leads to:

$$\theta = A/A_M = \exp[\Delta S^\circ/R] \exp[-\Delta H^\circ/RT]\, p/\{1 + \exp[\Delta S^\circ/R] \exp[-\Delta H^\circ/RT]\, p\} \qquad (2.6)$$

Eqn (2.6) describes the expected temperature and pressure dependence of the intensity of the relevant IR absorption band, as a function of the parameters ΔS°, ΔH° and A_M.

Strictly speaking, pressure, coverage and temperature are not independent; since they are related by an overall state

equation, implying mass partition between the adsorbed and the gas phase within a fixed volume, V_g:

$$N_{tot} = N + N_g \quad (2.7)$$

N_{tot} being the total number of adsorbate moles in the system, N that of adsorbed moles, and N_g the number of moles in the gas phase. However, interdependency among the above parameters does not affect results of the VTIR method, since the three parameters are independently measured.

Three cases may occur when applying eqn (2.6). The first case corresponds to a situation where the coverage θ is negligible ($\theta \ll 1$), and the vast majority of molecules are in the gas phase. Then:

$$A \approx A_M \exp[\Delta S^\circ/R] \exp[-\Delta H^\circ/RT]\, p \quad (2.8)$$

Moreover, because of the gas law:

$$pV_g = N_g RT \approx N_{tot} RT \quad (2.9)$$

As a consequence:

$$A \approx A_M \exp[\Delta S^\circ/R]\, N_{tot}(RT/V_g) \exp[-\Delta H^\circ/RT] \propto T \exp[-\Delta H^\circ/RT] \quad (2.10)$$

The intensity, A, decays exponentially with increasing temperature (mitigated by the multiplying factor T), and the pressure does not feature any longer. Hence, only ΔH° can be evaluated (see Section 5).

When experimental measurements cover a large θ range and the pressure values are available, two cases can occur. Either A_M is accurately known, so that θ is directly measurable, or only an approximate value (*e.g.* a lower limit) of A_M is available. In the former case, eqn (2.6) transforms into:

$$\ln \{\theta/[(1 - \theta)p]\} = (\Delta S^\circ/R) - (\Delta H^\circ/RT) \quad (2.11)$$

which gives direct access to both ΔS° and ΔH° (see Section 3).

When A_M is not accurately known, eqn (2.6) may be written as:

$$\ln \{A/[(A_M - A)p]\} = (\Delta S^\circ/R) - (\Delta H^\circ/RT) \quad (2.12)$$

which includes A_M as a non-linear parameter. In this case, a refined value of A_M can be obtained by an iteration procedure which involves discrete changes of the starting (approximate) value of A_M at each stage, and linear regression of eqn (2.12), until the best fit is obtained (see Section 4).

Finally, some critical points involved in the VTIR method merit further comment. One basic assumption is validity of the Lambert–Beer law (LBL) according to which the number of species showing IR absorption at any given frequency is proportional to the absorbance measured at that frequency. This is not the case when there is strong intermolecular coupling among adsorbed species, for instance in the case of CO adsorbed on metals.[10] Hence, in such cases the VTIR method (as discussed here) cannot be used. Validity of the LBL for IR spectra of adsorbed species has also been questioned[11] for systems exhibiting strong light scattering. Reference, however, to the changes in specific absorbance rated to background should minimize this inconvenience. A more fundamental objection is that IR absorbing species, which should differ only in concentration for LBL to apply, can indeed change their nature during measurements; because the gas phase surrounding them reaches an increasing density along the adsorption experiment. It may thus be assumed, in principle, that direct application of LBL is never entirely correct. The point, however, is how meaningful deviations are. Evidence gathered on this point suggests that, the above considerations notwithstanding, LBL can be safely used. Indeed: (*i*) results obtained by using the VTIR method show a remarkable agreement with independently derived data, and (*ii*) consistent results were obtained when the VTIR method was applied to IR bands occurring (for the same system) at widely different frequencies; *e.g.* for nitrogen adsorbed on H-ZSM-5 (Section 3) and for CO on H–Y zeolites.[9]

Use of the van't Hoff relationship for deriving thermodynamic quantities can have drawbacks when the temperature range is small, *e.g.* a spurious correlation between ΔH° and ΔS° can appear.[12,13] It is remarkable that this criticism does not apply to the VTIR method. By using the variable temperature IR cell as a closed system, the temperature range over which adsorption can be observed is substantially enlarged (as explained above) and this contributes to enhance the reliability of the method.

It should also be pointed out that when applying the van't Hoff eqn (2.2), the implicit assumption is made (as usual) that both ΔH° and ΔS° are temperature independent. This implies that Δc_p°, the difference in specific heat at constant pressure between the gas phase and the adsorbed phase in standard conditions, is nil (see also Section 6). Strictly speaking, this condition is never fulfilled, because the degrees of freedom of the molecule in the two states are different: in particular, translational degrees of freedom in the gas phase are replaced by low-lying vibrational ones in the adsorbed state. However, this also means that Δc_p° may be estimated not to exceed a few ½ R units; which should not affect significantly the final results.

3 Nitrogen adsorption on H-ZSM-5

The system N_2/H-ZSM-5 affords an example where both, the adsorbed molecule and the zeolite adsorbing centre, show a characteristic IR absorption band which can be used for thermodynamic studies of the gas–solid interaction. As a rule, zeolites in their protonic (acid) form invariably show IR absorption bands arising from the Brønsted acid Si(OH)Al hydroxy groups. These bands can appear in two different wavenumber ranges: 3650–3600 and 3580–3530 cm^{-1}. The high-frequency range corresponds to Brønsted acid OH groups vibrating inside large cavities, while in smaller voids the low-frequency range is observed.[14] However, these small voids (formed by less than eight-membered rings) are not usually accessible to adsorbed molecules.

The blank IR spectrum of an H-ZSM-5 zeolite (Si : Al = 25 : 1) outgassed at 725 K is shown in Fig. 1a. The Brønsted acid O–H stretching band appears at 3616 cm^{-1}, while the

weak one seen at 3747 cm^{-1} corresponds to silanols. Upon adsorption of nitrogen (*ca.* 10 Torr at room temperature) by the zeolite wafer, the silanol band was not significantly altered. However, the O–H band corresponding to Brønsted acid sites was found to decrease to an extent which was a function of temperature.[8] Simultaneously, a new (broader) band, from hydrogen bonded $OH\cdots N_2$ species, appeared at about 3500 cm^{-1}. This is shown in Fig. 1b, which depicts some variable-temperature IR spectra plotted in the difference mode (*i.e.*, after subtracting the zeolite blank spectrum). A further consequence of the formation of $OH\cdots N_2$ adducts is the activation (in the IR) of the fundamental N–N stretching mode of the adsorbed dinitrogen molecules. The corresponding IR absorption band appears at 2331 cm^{-1}, and shows a temperature-dependent intensity which reflects that of the O–H stretching band at 3616 cm^{-1} (Fig. 1c).

Presence of suitable IR absorption bands coming from both the adsorption site and the adsorbed molecule can be expected (in general) when dealing with protonic zeolites. This is at variance to the case of cationic zeolites, for which the adsorption site does not display a characteristic band suitable for studying adsorption thermodynamics. For protonic zeolites, it should also be noted that application of the VTIR method to the O–H stretching band facilitates direct knowledge of coverage. At any given temperature and (adsorbed) gas equilibrium pressure, the fraction $1 - \theta$ of empty adsorbing sites can be directly obtained by dividing the corresponding OH band intensity by its maximum value; *i.e.* that shown by the blank zeolite spectrum.

The variable temperature IR spectra depicted in Fig. 1b were selected from a much larger series of measurements[8] covering a temperature range from about 100 to 185 K. From the whole series of spectra (corresponding to the OH band) the plot of eqn (2.11) shown in Fig. 2 was obtained. This linear plot gave the values of $\Delta H^\circ = -19.7\ (\pm 0.5)$ kJ mol^{-1} and

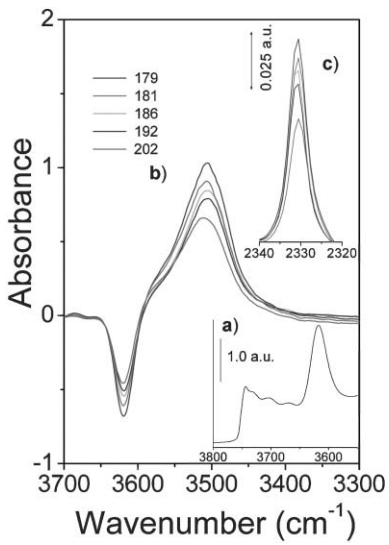

Fig. 1 (a) Blank spectrum of an H-ZSM-5 zeolite, showing the Brønsted acid OH band at 3616 cm^{-1}; (b) difference IR spectra (zeolite blank subtracted) in the O–H stretching region after dosing with nitrogen, showing variation with temperature; (c) N–N stretching region. Temperature, in K, as shown.

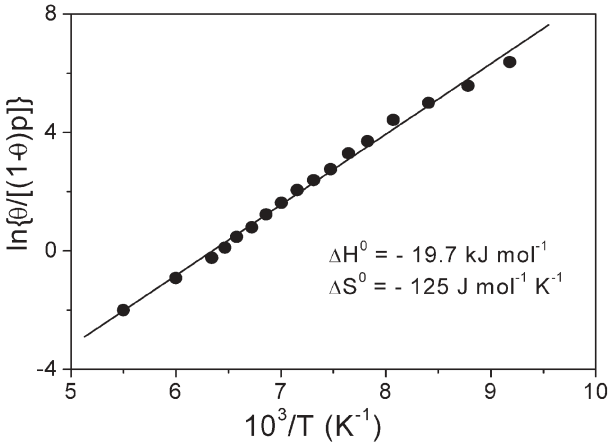

Fig. 2 Plot of the left-hand side of eqn (2.11) *versus* reciprocal temperature, for the OH band (Fig. 1a) of H-ZSM-5 having adsorbed nitrogen.

$\Delta S^\circ = -125\ (\pm 5)$ J mol^{-1} K^{-1} for the adsorption enthalpy and entropy (respectively) of dinitrogen adsorbed on H-ZSM-5. As a test, parallel calculations using eqn (2.12) were performed on the set of data corresponding to the N–N stretching band, at 2331 cm^{-1} (Fig. 1c); these calculations gave the same ΔH° and ΔS° values as above (within the stated error limits). It is also relevant to point out that Savitz *et al.*[15] studied the N_2/H-ZSM-5 system using adsorption microcalorimetry, at 195 K. Although these authors concluded that the interaction between dinitrogen and the Brønsted acid sites was too weak to be accurately measured, the fact is that an adsorption heat of about 19 kJ mol^{-1} can be derived from their reported measurements. This (approximate) microcalorimetric result is very close to the ΔH° value of $-19.7\ (\pm 0.5)$ kJ mol^{-1} obtained by the VTIR method. On the other hand, density functional quantum chemical calculations on the interaction of dinitrogen with the cluster model $H_3Si(OH)AlH_3$ are also available.[16] The calculated binding energy is 10.6 kJ mol^{-1}. This lower value, as compared to 19.7 kJ mol^{-1}, should be somewhat expected; since the acidity of the hydroxyl group in the cluster model is known to be significantly smaller than that of the real Brønsted acid sites of zeolites.[17]

In summary, two main points can be remarked from the foregoing overview of VTIR spectroscopy applied to the N_2/H-ZSM-5 system. First, it gives an example of how an IR absorption band characterizing the adsorption site can advantageously be used for studying adsorption thermodynamics. Secondly, the ΔH° value obtained from variable-temperature IR spectroscopy was found to agree with corresponding data derived from both adsorption microcalorimetry and quantum chemical calculations; and this constitutes a satisfactory test for the VTIR method. Further support comes from other thermodynamic studies reviewed below.

4 Hydrogen adsorption on zeolites

Infrared spectra of molecular hydrogen adsorbed at 77 K on alkali-metal exchanged zeolites are known to show a main absorption band in the region 4070–4100 cm^{-1}, which

corresponds to the fundamental H–H stretching mode of adsorbed dihydrogen. Perturbation of the H_2 molecule by the zeolite adsorbing centres (exchangeable cations and nearby oxygen anions of the zeolite framework) renders the H–H mode IR active and brings about a bathochromic shift from the (Raman active) gas phase value of 4136 cm^{-1}. An example[18] is depicted in Fig. 3, where some variable-temperature IR spectra of dihydrogen adsorbed on the zeolite Na-ZSM-5 are shown; the H–H band is seen at 4101 cm^{-1}. In this case, however, eqn (2.11) cannot be directly used, since previous knowledge of A_M is needed in order to convert absorbance (integrated band intensity) into the corresponding θ value. A starting value of $A_M = 3.64$ cm^{-1} was obtained[18] by running spectra corresponding to increasing hydrogen doses (equilibrium pressure) at 77 K and extrapolating the resulting isotherm. This starting value was refined by plotting the left hand side of eqn (2.12) against reciprocal temperature for A_M values, changed in successive steps of 0.05 cm^{-1}, covering the range 3.64 $\pm$ 0.5 cm^{-1}. The best fit to the whole set of experimental results was found at $A_M = 3.50$ cm^{-1}. Fig. 4 shows the linear plot thus obtained for eqn (2.12). This linear plot leads to the values of $\Delta H^\circ = -10.3$ kJ mol^{-1} for the standard adsorption enthalpy, and $\Delta S^\circ = -121$ J mol^{-1} K^{-1} for the corresponding entropy change. The estimated error limits were of about ± 0.5 kJ mol^{-1} for enthalpy and ± 10 J mol^{-1} K^{-1} for entropy. Regarding adsorption enthalpy, the value of 10.3 kJ mol^{-1} is consistent with that of about 8 kJ mol^{-1} found by Basmadjian[19] for the isosteric heat of adsorption of dihydrogen on Na–A zeolites, thus providing a further satisfactory test for the VTIR method. Note that, because of a higher coordination number of the Na^+ ion in Na–A, the interaction energy with the adsorbed dihydrogen molecule is expected to be smaller in the H_2/Na–A system, as compared to that of H_2/Na-ZSM-5.

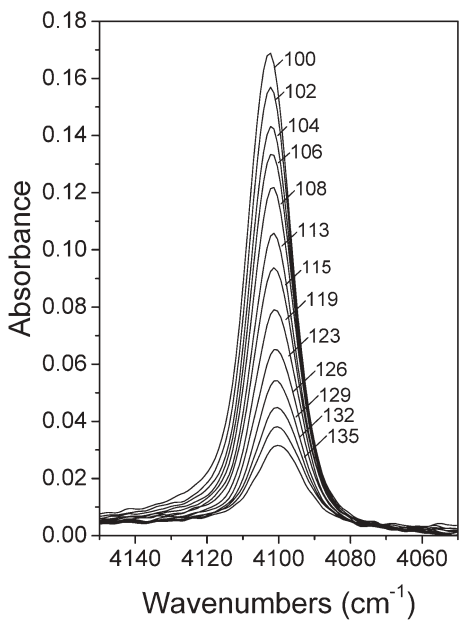

Fig. 3 Difference IR spectra (zeolite blank subtracted) in the H–H stretching region for dihydrogen adsorbed on Na-ZSM-5. Temperature, in K, as shown (more details can be found in ref. 18).

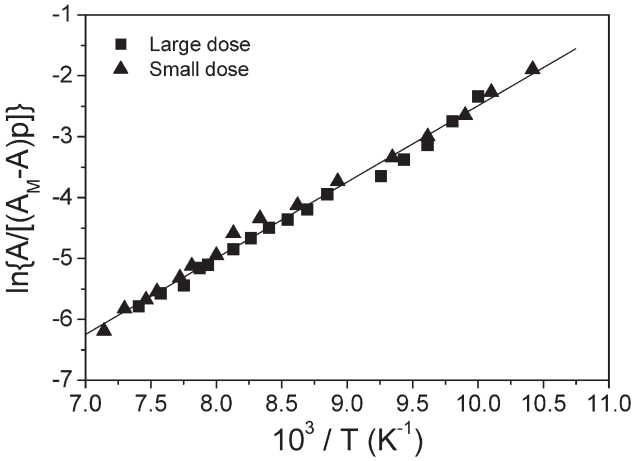

Fig. 4 Plot of the left-hand side of eqn (2.12) *versus* reciprocal temperature for dihydrogen adsorbed on Na-ZSM-5. Experimental results corresponding to a large (*ca.* 50 Torr at room temperature) and to a small (*ca.* 20 Torr) hydrogen dose are shown.

By comparing the adsorption enthalpy value of -10.3 kJ mol^{-1} with the liquefaction enthalpy of hydrogen (at 20.45 K), which amounts to -0.90 kJ mol^{-1}, it turns out that the energy involved in the adsorption process on Na-ZSM-5 is significantly larger than that corresponding to liquefaction, and this is a favourable feature regarding the potential of zeolites as adsorbents for cryogenic hydrogen storage in pressurised vessels. It is also worth adding that parallel measurements on the H_2/Li-ZSM-5 and H_2/K-ZSM-5 systems yielded ΔH° values of -6.5 (± 0.5) and $-9.1(\pm 0.5)$ kJ mol^{-1}, respectively.[18,20]

Regarding entropy change upon adsorption, the value of $\Delta S^\circ = -121(\pm 10)$ J mol^{-1} K^{-1}, found for H_2 on Na-ZSM-5, should be compared with the absolute entropy of dihydrogen, which amounts to 163 J mol^{-1} K^{-1}, at the representative temperature of 100 K and the standard pressure of 1 Torr.[20] It turns out that the standard entropy of the adsorbed phase is of about 40 J mol^{-1} K^{-1}. Qualitatively, this result suggests a substantial freedom of the adsorbed dihydrogen molecules, which is likely to reflect transformation of translational modes into low-lying vibrational modes, with preservation (at least to a large extent) of rotational freedom.

5 CO adsorption on zeolites: formation of 1 : 1 and 1 : 2 cation–CO adducts

When adsorbed (at a low temperature) on alkali-metal-exchanged zeolites, CO forms M^+–CO and M^+–OC species (M = alkali metal); similarly, on zeolites containing alkaline-earth cations, the corresponding M^{2+}–CO and M^{2+}–OC species are formed. The C-bonded species have been termed[21] *nonclassical metal carbonyls*, since they do not conform to the classical chemical bond description which involves carbon monoxide acting simultaneously as an electron σ-donor and π-acceptor ligand for the metal. This synergistic bonding usually leads to a larger C–O distance, and a lower C–O

vibration frequency, for the metal carbonyl as compared to the free CO molecule. By contrast, cationic M^+–CO and M^{2+}–CO species of alkali and alkaline-earth metals in zeolites invariably show an IR absorption band upward shifted with respect to the 2143 cm^{-1} value of free carbon monoxide. M^+–OC and M^{2+}–OC species show, however, a bathochromic shift of the C–O stretching frequency (see Section 6).

Besides monocarbonyls, dicarbonyl $Na(CO)_2^+$ and $Li(CO)_2^+$ species have also been documented for CO adsorbed on Na–Y[22] and Li-ZSM-5 zeolites,[23] as well as $Ca(CO)_n^{2+}$ (n = 1–3) species[24] for CO adsorbed on Ca–Y. Relevant thermodynamic aspects of formation of C-bonded non-classical (cationic) monocarbonyls and their conversion into dicarbonyls are discussed below, while O-bonded species will be reviewed in Section 6.

Detailed experimental measurements[25] for CO adsorbed on the faujasite-type zeolite Sr–Y provide an example to illustrate (C-bonded) carbonyl and dicarbonyl species. Fig. 5 shows IR spectra obtained, at the fixed temperature of 77 K, by exposing Sr–Y to an increasing (equilibrium) pressure of CO; from about 0.5 up to 5 Torr. At the lowest CO dose, a main IR absorption band is seen at 2191 cm^{-1}. Upon increasing CO dosage, this band gradually shifts to lower wavenumber values without showing any discontinuous step. In agreement with available literature on CO adsorbed on alkali- and alkaline-earth-exchanged zeolites, this band is assigned to the fundamental C–O stretching mode of carbon monoxide in C-bonded $Sr(CO)_n^{2+}$ carbonyls, where the number of CO ligands increases (as frequency of the band decreases) from 1 to 2, and possibly 3.[24,25] For weakly bound CO, each ligand in a polycarbonyl behaves as an independent oscillator and only a single C–O stretching band is expected regardless of the corresponding geometry; this band, however, shifts to lower frequency when the same Sr^{2+} ion is shared by an increasing

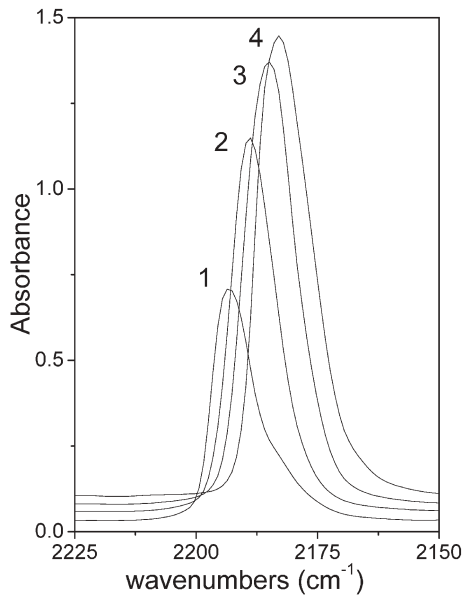

Fig. 5 Infrared spectra in the C–O stretching region of carbon monoxide adsorbed on Sr–Y at 77 K and increasing dosage: (1) 0.5, (2) 2, (3) 4 and (4) 5 Torr. The zeolite blank was subtracted.

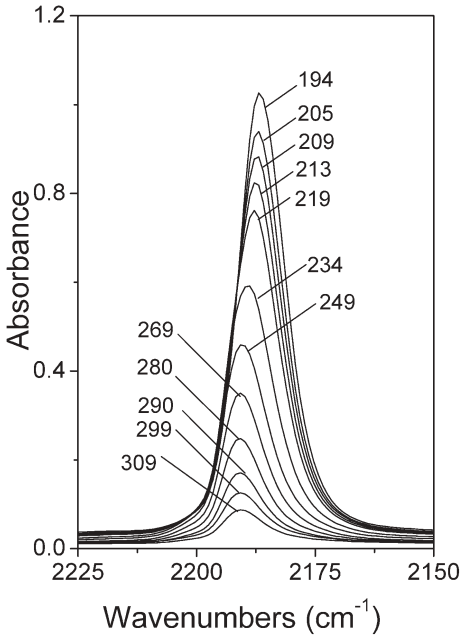

Fig. 6 Variable temperature IR spectra of CO (*ca.* 4 Torr) adsorbed on Sr–Y. Temperature, in K, as shown.

number of CO ligands. VTIR spectra covering a wide temperature range are shown in Fig. 6. Only one peak is visible, the frequency of which is constant at 2187 cm^{-1} up to 205 K and then it shifts steadily to 2191 cm^{-1}. The band at 2187 cm^{-1} was assigned to the C–O stretching mode of the dicarbonyl species $Sr(CO)_2^{2+}$, while that at 2191 cm^{-1} should correspond to the C–O stretching of the monocarbonyl $Sr(CO)^{2+}$.

Fig. 7 reports peak position *versus* integral area for the main IR adsorption band in all of the VTIR spectra recorded.[25] The two plateaus observed correspond, respectively, to the regions where monocarbonyl (left-hand side) and dicarbonyl (right-hand side) species predominate. The sloping segment in Fig. 7 corresponds to spectra which have a substantial contribution from both, mono- and dicarbonyl species. The region up to 5 cm^{-1} of integrated band intensity corresponds to formation

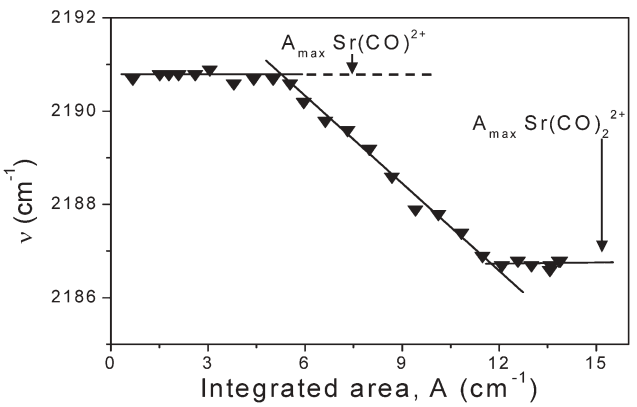

Fig. 7 Wavenumber of peak maxima *versus* integrated band intensity for CO adsorbed, at variable temperature, on Sr–Y (details can be found in ref. 25).

of the monocarbonyl from empty Sr^{2+} sites and adsorbed CO, following the process,

$$Sr^{2+} + CO_{(g)} \rightleftarrows Sr(CO)^{2+} \quad (5.1)$$

Similarly, the region having integrated intensity larger than 12 cm^{-1} represents formation of dicarbonyls from monocarbonyls, in the absence of empty Sr^{2+} sites:

$$Sr(CO)^{2+} + CO_{(g)} \rightleftarrows Sr(CO)_2{}^{2+} \quad (5.2)$$

Thermodynamics of the equilibrium processes described by eqn (5.1) and (5.2) can be analysed as follows. Let θ_0, θ_1 and θ_2 be the coverages of bare cations, monocarbonyl and dicarbonyl species, respectively. The dependence of the integrated intensity of the 2191 cm^{-1} band (A_{2191}) on temperature and pressure can be described by eqn (5.3) below, which has the same nature as eqn (2.12):

$$\theta_1/[(1 - \theta_1)p] = \exp(\Delta S^\circ_m/R)\exp(-\Delta H^\circ_m/RT) \quad (5.3)$$

with $\theta_1 = A_{2191}/A^M{}_{2191}$, where $A^M{}_{2191}$ is the integrated intensity corresponding to full coverage of monocarbonyls, $\theta_1 = 1$, and ΔH°_m and ΔS°_m refer to the formation of monocarbonyl species, eqn (5.1). Eqn (5.3) can be linearised as:

$$\ln\{\theta_1/[(1 - \theta_1)p]\} = (\Delta S^\circ_m/R) - (\Delta H^\circ_m/RT) \quad (5.4)$$

The actual value of $A^M{}_{2191}$ needed to apply eqn (5.4) is not known from experimental measurements. Experimentally, the maximum absorbance value of the monocarbonyl was found to be 5.02 cm^{-1}. However, this value does not correspond to full coverage ($\theta_1 = 1$) since that coverage could not be obtained before dicarbonyl species started to form.[25] A refined value of $A^M{}_{2191} = 7.0$ cm^{-1} was obtained by a trial and error fit of eqn (5.4) to the corresponding experimentally determined points. Such a value is indicated in Fig. 7 by a vertical arrow. From the linear plot thus obtained, the corresponding values of standard enthalpy and entropy for monocarbonyl formation were found to be $\Delta H^\circ_m = -45.3$ kJ mol^{-1} and $\Delta S^\circ_m = -179$ J mol^{-1} K^{-1}, respectively.

No calorimetric measurements seem to be available on the CO/Sr–Y system, so that the standard enthalpy of formation of the $Sr(CO)^{2+}$ monocarbonyl obtained by using the VTIR method cannot be checked against direct evaluations. However, the value of -45.3 kJ mol^{-1} appears to be quite reasonable on the following grounds. First, the standard enthalpy of formation of $Ca(CO)^{2+}$ species for CO adsorbed on a Ca–Y zeolite has been measured[26] (by adsorption calorimetry) to be -50 kJ mol^{-1}; the corresponding value for $Sr(CO)^{2+}$ is expected to be somewhat lower, because of the smaller polarising power of the Sr^{2+} cation, as compared to Ca^{2+}. Secondly, from an empirical relationship[27] between heat of adsorption of CO and the corresponding stretching frequency (for a set of non-*d* cations) an approximate value of about 48 kJ mol^{-1} can be derived for a C–O stretching frequency of 2191 cm^{-1}.

The thermodynamic parameters related to eqn (5.2), which describes formation of $Sr(CO)_2{}^{2+}$ from the corresponding monocarbonyl and CO, can be obtained by following a procedure similar to the one above; applying eqn (5.5) below instead of (5.4):

$$\ln\{\theta_2/[(1 - \theta_2)p]\} = (\Delta S^\circ_d/R) - (\Delta H^\circ_d/RT) \quad (5.5)$$

However, the relationship between θ_2 and the measured integrated intensity of the band at 2187 cm^{-1}, A_{2187}, is more complex because both mono- and dicarbonyl species contribute to such an integrated intensity. It can be shown[25] that the corresponding value of θ_2 is given by:

$$\theta_2 = (A_{2187} - A^M{}_{2191})/(A^M{}_{2187} - A^M{}_{2191}) \quad (5.6)$$

where $A^M{}_{2187}$ is the intensity corresponding to $\theta_2 = 1$, a situation again not actually reached. The required value of $A^M{}_{2187}$, which has to be higher than the highest value of absorbance reported in Fig. 7 (13.5 cm^{-1}), was again obtained by a best fit criterion. A value of $A^M{}_{2187} = 15.0$ cm^{-1} (indicated in Fig. 7 by a vertical arrow) gave a very satisfactory straight line for the plot concerning eqn (5.5); from which the enthalpy and entropy changes involved in formation of the dicarbonyl from the monocarbonyl and adsorbed CO (eqn (5.2)) were found to be $\Delta H^\circ_d = -30.2$ kJ mol^{-1} and $\Delta S^\circ_d = -138$ J mol^{-1} K^{-1}, respectively. Again, the enthalpy of formation of the dicarbonyl species cannot be compared with any direct experimental estimate: the obtained value, however, appears to be reasonable, since as a smaller value than that of monocarbonyl species is expected.

The above values of standard enthalpy and entropy change for the CO/Sr–Y system can be compared with a set of calorimetrically determined data[28] for CO adsorbed on several metal oxides, and on the zeolite Na-ZSM-5. This comparison is made in Fig. 8, which shows a linear correlation between $\log(-\Delta S^\circ)$ and $\log(-\Delta H^\circ)$ for several CO/adsorbent systems. It is seen that the values of the thermodynamic parameters derived for the CO/Sr–Y system satisfactorily fit into the

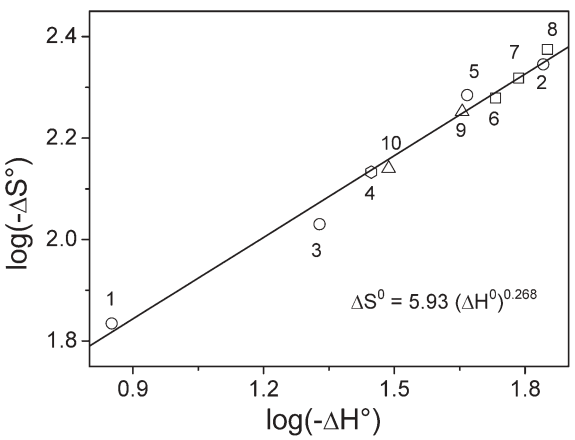

Fig. 8 Correlation between ΔS° and ΔH° for CO adsorbed on: (1) alumina (weak Lewis site); (2) alumina (strong Lewis site); (3) silica-supported (reduced) chromia; (4) Na-ZSM-5; (5) zinc oxide; (6) titania (strong Lewis site); (7) titania (intermediate site); (8) titania (strong Lewis site); (9) CO/Sr–Y monocarbonyl; and (10) CO/Sr–Y dicarbonyl. Details can be found in ref. 25.

correlation, which lends further support to the method used. It is worth adding that the obtained $A^{M}{}_{2187}$ value (13.5 cm^{-1}) is about twice the value of $A^{M}{}_{2191}$ (7.0 cm^{-1}) thus showing that the molar absorption coefficient of CO is nearly the same in the monocarbonyl and dicarbonyl species.

As a further illustration of the capabilities of the VTIR method, let us consider the CO/Na-ZSM-5 system. Variable temperature IR spectra of CO adsorbed on Na-ZSM-5 have been reported in the literature[29] but no corresponding values of equilibrium pressure are available. However, by applying eqn (2.10) to spectra corresponding to a relatively high temperature range (*i.e.* to the lowest coverages) an approximate value of ΔH° can be derived. Fig. 9 reports such spectra, which show the C–O stretching band at 2178 cm^{-1}. The inset in Fig. 9 shows the logarithm of the intensity of this band, after dividing by the absolute temperature T, plotted against $1/T$. A correlation is observed. Points corresponding to the highest temperature range do fall on a straight line, from which a value of $\Delta H^{\circ} = -27.6\ (\pm 0.8)$ kJ mol^{-1} can be derived. As expected, at a higher coverage (lower temperature) a progressive deviation is seen; since eqn (2.10) does not hold any longer. However, the important point is that the calculated value of $\Delta H^{\circ} = -27.6$ kJ mol^{-1} practically coincides with that of $\Delta H^{\circ} = -28$ kJ mol^{-1} obtained by a direct calorimetric measurement on the CO/Na-ZSM-5 system.

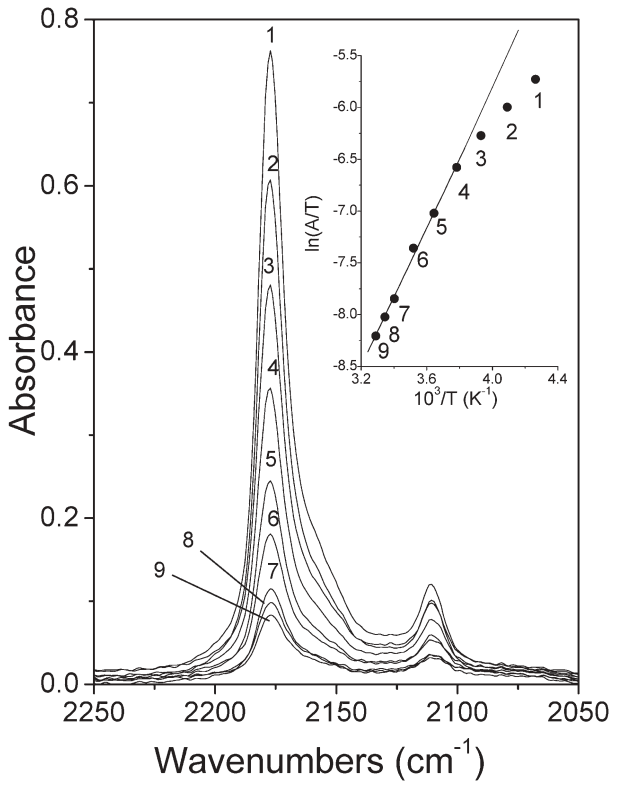

Fig. 9 Intensity variation of the C–O stretching band (at 2178 cm^{-1}) for the $Na(CO)^{+}$ species of CO adsorbed on Na-ZSM-5. Fixed dose (*ca.* 0.8 Torr) of CO at increasing temperatures, in K, as follows: (1) 234.7, (2) 244.5, (3) 254.5, (4) 264.5, (5) 274.5, (6) 284.3, (7) 294.0, (8) 299.0, and (9) 304.0.

6 Thermal equilibrium between C-bonded and O-bonded cationic alkali-metal carbonyls

As already pointed out in Section 5, infrared spectra of carbon monoxide adsorbed on alkali-metal-exchanged zeolites invariably show a main IR absorption band upward shifted with respect to the 2143 cm^{-1} value of free CO. Thus, for the whole series of M^{+}-ZSM-5 zeolites (M = Li, Na, K, Rb, Cs), this cation-specific high frequency (HF) band was observed[29–32] at a wavenumber which gradually increases from 2157 cm^{-1} for Cs^{+} up to 2195 cm^{-1} for Li^{+}. The specific wavenumber value for each cation is a linear function of the corresponding electric field,[31] thus strongly suggesting that the M^{+}–CO bond is primarily electrostatic in nature. Besides the HF band, a less intense low frequency (LF) band was also frequently observed,[29] in the IR spectra of CO adsorbed on alkaline zeolites. This LF band, which appears below 2143 cm^{-1}, is also cation-specific; for the M^{+}-ZSM-5 series, it was observed at wavenumbers gradually increasing from 2100 cm^{-1} for Li^{+} up to 2112 cm^{-1} for Cs^{+}. Both, experimental results[29–33] and quantum-chemical calculations[30,34] show that the LF band originates from the C–O stretching mode of O-bonded CO in M^{+}–OC species, while the HF band is due to C-bonded M^{+}–CO adducts. Variable-temperature IR spectroscopy was used to demonstrate that, for any given alkali-metal ion, the carbonyl, $M(CO)^{+}$, and isocarbonyl, $M(OC)^{+}$, species are in *thermal equilibrium*.[29,35] Further studies of this finding are relevant, not only to the coordination chemistry of the CO ligand, but also to fundamental studies of the chemical bond in a broader scope.

Isocarbonyl, $M(OC)^{+}$, species are less stable than the corresponding carbonyls, $M(CO)^{+}$; as deduced from both, quantum-chemical calculations,[34,36] and experimental evidence[29,35] which show that population of isocarbonyls is always much smaller than that of carbonyls. Variable-temperature IR spectroscopy is currently being used to determine the magnitude of the enthalpic change involved in the carbonyl–isocarbonyl isomerization process; and hence, the relative stability of the involved chemical species. Both, the strategy and recent developments in this active research field will now be reviewed.

Referring to CO adsorbed on alkali-metal exchanged zeolites, let us consider the isomerization equilibrium between carbonyl, $M(CO)^{+}$, and isocarbonyl, $M(OC)^{+}$, cationic species given by eqn (6.1) below:

$$ZM(CO)^{+} \rightleftarrows ZM\ (OC)^{+} \qquad (6.1)$$

where M is an alkali metal and Z stands for the zeolite framework. Because of the lesser stability of isocarbonyls as compared to corresponding carbonyls, eqn (6.1) implies an endothermic process; at variance with the adsorption processes described in the preceding sections, which are invariably exothermic.

For any given temperature, the equilibrium constant, K, of eqn (6.1) is simply the ratio θ_{OC}/θ_{CO}, where θ_{OC} and θ_{CO} are the fractional coverages of O-bonded and C-bonded CO adducts which give rise (respectively) to the LF and HF IR absorption bands described above. If A_{LF} and A_{HF} are the

integrated intensities of these IR bands, and ε_{LF} and ε_{HF} the corresponding molar absorption coefficients, we have:

$$K = (A_{LF}/A_{HF})\ (\varepsilon_{LF}/\varepsilon_{HF}) \quad (6.2)$$

The temperature dependence of the equilibrium constant, K, is given by the van't Hoff eqn (2.2) which, when combined with eqn (6.2) yields:

$$\ln\ (A_{LF}/A_{HF}) = (-\Delta H^{\circ}/RT) + (\Delta S^{\circ}/R) + \ln\ (\varepsilon_{LF}/\varepsilon_{HF}) \quad (6.3)$$

Hence, by measuring the intensity ratio A_{LF}/A_{HF} over a wide temperature range, the corresponding linear plot of ln (A_{LF}/A_{HF}) *versus* $1/T$ gives direct access to the isomerization enthalpy, ΔH°, between carbonyl and isocarbonyl species; knowledge of molar absorption coefficients is not needed. Note that, because of the positive value of ΔH°, the equilibrium constant, K, increases with increasing temperature; as always happens for endothermic reactions.

As already pointed out in Section 2, the above strategy makes the implicit assumption that ΔH° and ΔS° are, at least approximately, temperature independent. This is equivalent to assume that Δc_p° (the variation of specific heat between carbonyl and isocarbonyl species) is negligible; since Δc_p°, ΔH° and ΔS° are related by the well known Kirchhoff eqn (6.4) and (6.5) below:

$$d\Delta H^{\circ}/dT = \Delta c_p^{\circ}\ (T) \quad (6.4)$$

$$d\Delta S^{\circ}/dT = \Delta c_p^{\circ}\ (T)/T \quad (6.5)$$

Computational results on model systems[36] have indeed shown that Δc_p° for the equilibrium process described by eqn (6.1) is negligible. Hence, application of eqn (6.3) over a relatively large temperature range seems to be justified.

As an example, Fig. 10 shows some selected VTIR spectra of CO adsorbed on Na-ZSM-5. They were taken[29] by dosing the zeolite wafer with about 0.8 Torr of CO at 77 K, after which the IR cell was closed and IR spectra were run at 2–5 K intervals, from 77 K up to room temperature. The HF band, corresponding to $Na(CO)^+$ species, is seen at 2178 cm^{-1}, while the LF band ($Na(OC)^+$ species) appears at 2112 cm^{-1}. The weak band observed at about 2129 cm^{-1} is the ^{13}C (natural abundance 1.1%) counterpart of the HF band, which is of no concern here. The behaviour of the HF band at low coverages (*i.e.*, in the highest temperature range) has already been reported in Fig. 9; to illustrate the method for evaluating the adsorption enthalpy when values of equilibrium pressure are not available.

Fig. 10 clearly shows that at the lowest temperature the HF band is much more intense than the LF band, reflecting the higher stability of the $Na(CO)^+$ carbonyl as compared to the $Na(OC)^+$ isocarbonyl species. However, when temperature is raised, the LF band starts to increase, at the expense of the HF band. This is precisely the behaviour to be expected from the endothermic process described by eqn (6.1). At a higher temperature (Fig. 10) both bands decrease rapidly, because the net amount of adsorbed CO decreases. However, the intensity ratio A_{LF}/A_{HF} was found to increase monotonically with increasing temperature for a large series of IR spectra[29] taken over a temperature range going from 77 to 304 K. From these

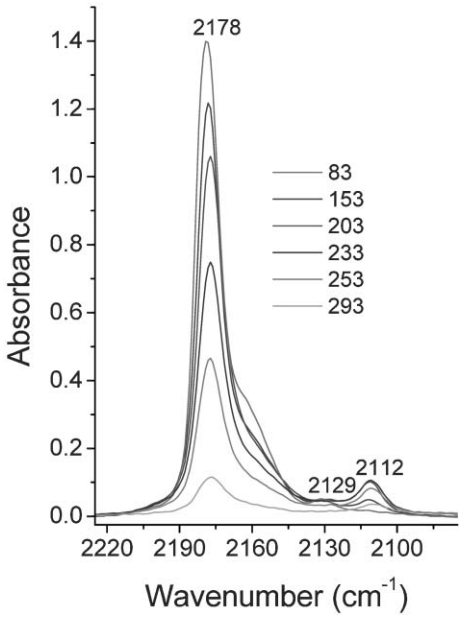

Fig. 10 Variable temperature FTIR spectra of CO (*ca.* 0.8 Torr) adsorbed on Na-ZSM-5 (temperature, in K, as shown). Note that the 2178 cm^{-1} band steadily decreases as temperature is raised, whereas the 2112 cm^{-1} band first increases, then decreases.

spectra, the plot of ln (A_{LF}/A_{HF}) *versus* reciprocal temperature shown in Fig. 11 was obtained. This linear plot leads to the value of 3.8 kJ mol^{-1} for the enthalpy change involved in the isomerization process $ZM(CO)^+ \rightleftarrows ZM(OC)^+$ between carbonyl and isocarbonyl species. From parallel studies[33,35] on other alkali-metal exchanged zeolites, the experimental results shown in Table 1 were obtained. Also, quantum chemical calculations have been performed (at the B3-LYP level) on the

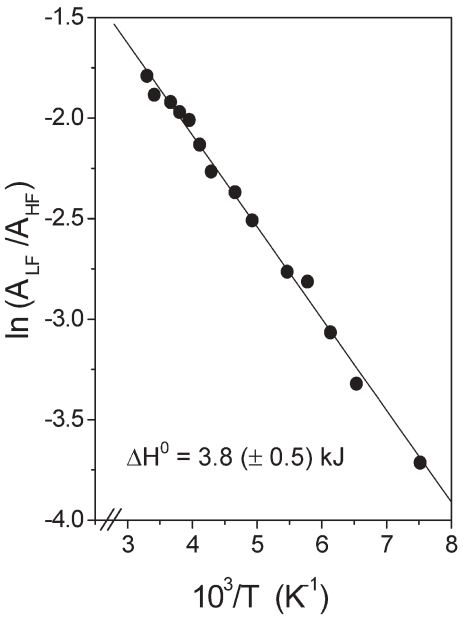

Fig. 11 Plot of the left-hand side of eqn (6.3) *versus* reciprocal temperature, used to derive the isomerization enthalpy between $Na(CO)^+$ and $Na(OC)^+$ species for CO adsorbed on the zeolite Na-ZSM-5 (ref. 29).

Table 1 Peak position (cm^{-1}), and enthalpy change (kJ mol^{-1}) in the isomerization process $M(CO)^+ \rightleftarrows M(OC)^+$, for CO adsorbed on several alkali-metal-exchanged zeolites

System	$\nu/M(CO)^+$	$\nu/M(OC)^+$	ΔH° (exp.)	ΔH° (calc.)[a]
CO/Li-ZSM-5	2195	2102	7.8	6.3
CO/Na-ZSM-5	2178	2112	3.8	5.6
CO/K-ZSM-5	2166	2117	3.2	2.9
CO/Rb-ZSM-5	2161	2120	1.8	2.5
CO/Cs-ZSM-5	2157	2122	—	2.1
CO/Na–Y	2171	2122	2.4	5.6

[a] $[AlH(OH)_3]^-M^+$ cluster model.

interaction of CO with the cluster model $[AlH(OH)_3]^-M^+$ (M = Li, Na, K, Rb, Cs), which was used to simulate cation sites in zeolites.[34] Values of ΔH°, the isomerization enthalpy between $M(CO)^+$ and $M(OC)^+$ species, obtained in these *ab initio* calculations are also given in Table 1. They are seen to show the same general trend as the corresponding experimental values. The isomerization enthalpy between carbonyl and isocarbonyl species decreases with decreasing charge to radius ratio of the alkali metal cation; a fact which was correlated (to a first approximation) to the corresponding magnitude of ion–dipole interaction.[33]

The carbonyl–isocarbonyl isomerization phenomenon takes place also when CO is adsorbed on zeolites containing alkaline-earth cations.[25] For CO adsorbed on the zeolite Sr–Y (discussed in Section 5 regarding formation of mono- and dicarbonyls) it was observed[25] that, besides the monocarbonyl species $Sr(CO)^{2+}$ absorbing at 2191 cm^{-1}, a rather weak band corresponding to the isocarbonyl species $Sr(OC)^{2+}$ appeared at 2095 cm^{-1}. For dicarbonyls, besides the species $Sr(CO)_2{}^{2+}$ characterized by a single mode at 2187 cm^{-1}, a weak band was also observed at 2098 cm^{-1} and ascribed to the species $[Sr(CO)OC]^{2+}$. A species having two isocarbonyl ligands is probably also formed, but its limited population precludes detection of the corresponding IR absorption mode.

The processes:

$$Sr(CO)^{2+} \rightleftarrows Sr(OC)^{2+} \quad (6.6)$$

$$Sr(CO)_2{}^{2+} \rightleftarrows [Sr(CO)OC]^{2+} \quad (6.7)$$

were studied,[25] (following a procedure similar to that adopted for characterizing formation of mono and dicarbonyls) in two separate regions of coverage; those corresponding to the two plateaus in Fig. 7. The isomerization enthalpy for the process described by eqn (6.6) resulted to be 9.8 kJ mol^{-1}, and that for eqn (6.7) is 7.6 kJ mol^{-1}. These data, combined with those discussed in Section 5, lead to the enthalpy level scheme depicted in the left-hand side of Fig. 12. The right-hand side gives the corresponding scheme for entropy, which is much simpler because isomerization does not bring about any entropy change. As a whole, Fig. 12 provides a fairly thorough thermodynamic characterisation of the CO/Sr–Y system.

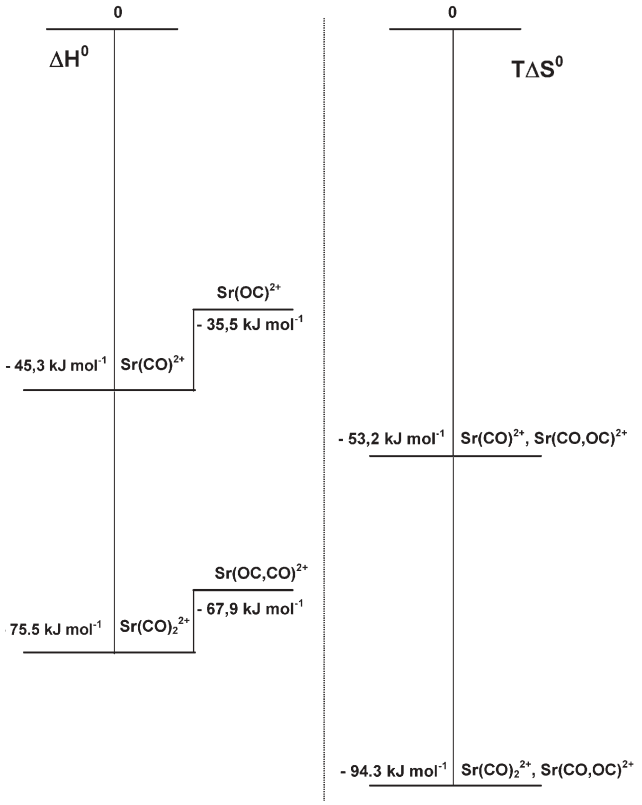

Fig. 12 Thermodynamic diagram for CO adsorbed on the faujasite-type zeolite Sr–Y. The left hand side shows the enthalpy levels, with respect to the separated reagents, of monocarbonyl, dicarbonyl and isocarbonyl species, while the right-hand side shows the corresponding entropy levels. Note that, in order to have a common scale, entropy values were multiplied by T (298 K).

7 Summary and outlook

Use of variable temperature infrared spectroscopy for studying the thermodynamics of weak solid–gas interactions has been critically reviewed. The examples analysed show how the fundamental relationship of thermodynamics described by the van't Hoff equation (widely used in several fields of physical chemistry) can be successfully applied to describe (adsorption) equilibrium processes taking place at the solid–gas interface. The full potential of the VTIR method is exploited by running infrared spectra over a wide temperature range, and simultaneously measuring IR absorbance, temperature and equilibrium pressure. However, several aspects of the gas–solid interaction, including an estimation of the interaction energy and a detailed characterization of (different) adsorption sites can be accessible (under favourable conditions) even without a precise knowledge of equilibrium pressure.

Precise thermodynamic characterization of solid–gas interactions should help to advance several fields of both, fundamental chemistry and technological applications. On the applied side, the search for more efficient adsorbents for gas sensing, separation and storage should benefit from a more detailed study of processes taking place at the solid–gas interface. And this involves such areas as work-place security, air pollution control and the energy sector, to mention only a few examples. Regarding fundamental knowledge, detailed studies on weak solid–gas interactions are relevant to a number of fields, including aspects of hydrogen bonding,[37–39] coordination chemistry[21,33] and surface phenomena in a broad

sense. In particular, it should be noted that linkage isomerism, as discussed for carbon monoxide adsorbed on zeolites, can be a more general phenomenon. Polar molecules interacting with (electrically charged) adsorbing centres can, in principle, form a variety of (adsorption) complexes. When different adsorbed states are separated by a small energy barrier, thermal isomerization can be expected. In fact, besides carbon monoxide, isomerization was recently reported[40] for thiophene interacting with surface silanol groups on silica, and it was also suggested[41] for NO adsorbed on Na^+ and K^+-exchanged ETS-10 molecular sieves. Variable temperature infrared spectroscopy has proved to be a powerful tool for all of the foregoing applications; and this is even more the case when experimental results are combined with knowledge gained from theoretical calculations.[30,33]

Finally, it should be noted that the VTIR approach to the study of solid–gas interactions is quite unrestrained, despite some assumptions involved: (*i*) validity of the Beer–Lambert law, (*ii*) approximate constancy of ΔH° and ΔS°, and (*iii*) nearly ideal nature of the gas adsorption process. This last requirement could appear to be rather restrictive, because most practical adsorbents are heterogeneous. However, heterogeneity in adsorption often arises from the presence of several types of adsorbing centres which do not show much mutual interference. In such a case, the VTIR method can still be used to analyse each type of adsorbing centre, thus yielding results superior to those obtained with all-encompassing classical methods. An example could be the reversible adsorption of ammonia on severely dehydrated silica. Room temperature calorimetric measurements showed a pronounced decrease of the differential heat of adsorption when coverage increases, thus suggesting a marked site heterogeneity;[42] however, IR spectra showed that isolated silanols (readily recognisable by their characteristic band at 3747 cm^{-1}) interact with ammonia in an ideal manner; a (local) Langmuir isotherm was observed.[43] This means that a constant ΔH° value should be expected. A fact that probably becomes blurred by concurrent (adventitious) phenomena in the calorimetric measurements. VTIR spectroscopy will, hopefully, help to clarify this and many other debated points on several solid–gas systems. By contrast, surface phenomena which (at the moment) appear to be beyond the potential of the VTIR method are those involving interaction among occupied surface sites (induced heterogeneity), for which local equilibrium isotherms are far more complex than those of a Langmuir type.

References

1 F. Rouquerol, J. Rouquerol and D. H. Everett, *Thermochim. Acta*, 1980, **41**, 311.
2 M. J. Blandamer, P. M. Cullis and P. T. Gleeson, *Chem. Soc. Rev.*, 2003, **32**, 264.
3 R. J. Cvetanovic and Y. Amenomiya, *Adv. Catal.*, 1967, **17**, 103.
4 O. Dulaurent and D. Bianchi, *Appl. Catal. A*, 2000, **196**, 271.
5 S. Derrouiche, P. Gravejat and D. Bianchi, *J. Am. Chem. Soc.*, 2004, **126**, 13010.
6 G. Spoto, E. N. Gribov, G. Ricchiardi, A. Damin, D. Scarano, S. Bordiga, C. Lamberti and A. Zecchina, *Progr. Surf. Sci.*, 2004, **76**, 71.
7 T. P. Beebe, P. Gelin and J. T. Yates, *Surf. Sci.*, 1984, **148**, 526.
8 C. Otero Areán, O. V. Manoilova, G. Turnes Palomino, M. Rodríguez Delgado, A. A. Tsyganenko, B. Bonelli and E. Garrone, *Phys. Chem. Chem. Phys.*, 2002, **4**, 5713.
9 C. Otero Areán, O. V. Manoilova, A. A. Tsyganenko, G. Turnes Palomino, M. Peñarroya Mentruit, F. Geobaldo and E. Garrone, *Eur. J. Inorg. Chem.*, 2001, 1739.
10 P. Hollins, *Surf. Sci. Rep.*, 1992, **16**, 53.
11 C. Morterra, G. Magnacca and V. Bolis, *Catal. Today*, 2001, **70**, 43.
12 A. K. Galwey, *Adv. Catal.*, 1977, **26**, 247.
13 G. C. Bond, M. A. Keane, H. Kral and J. A. Lercher, *Catal. Rev. Sci. Eng.*, 2000, **42**, 319.
14 A. Zecchina and C. Otero Areán, *Chem. Soc. Rev.*, 1996, **25**, 187.
15 S. Savitz, A. L. Myers and R. J. Gorte, *J. Phys. Chem. B*, 1999, **103**, 3687.
16 K. M. Neyman, P. Strodel, S. Ph. Ruzankin, N. Schlensog, H. Knözinger and N. Rösch, *Catal. Lett.*, 1995, **31**, 273.
17 I. N. Senchenya, E. Garrone and P. Ugliengo, *J. Mol. Struct. (THEOCHEM)*, 1996, **368**, 93.
18 C. Otero Areán, M. Rodríguez Delgado, G. Turnes Palomino, M. Tomás Rubio, N. M. Tsyganenko, A. A. Tsyganenko and E. Garrone, *Microporous Mesoporous Mater.*, 2005, **80**, 247.
19 D. Basmadjian, *Can. J. Chem.*, 1960, **38**, 141.
20 C. Otero Areán, O. V. Manoilova, B. Bonelli, M. Rodríguez Delgado, G. Turnes Palomino and E. Garrone, *Chem. Phys. Lett.*, 2003, **370**, 631.
21 A. J. Lupinetti and S. H. Strauss, *Progr. Inorg. Chem.*, 2001, **49**, 1.
22 K. Hadjiivanov and H. Knözinger, *Chem. Phys. Lett.*, 1999, **303**, 513.
23 C. Otero Areán, O. V. Manoilova, M. Rodríguez Delgado, A. A. Tsyganenko and E. Garrone, *Phys. Chem. Chem. Phys.*, 2001, **3**, 4187.
24 K. Hadjiivanov and H. Knözinger, *J. Phys. Chem. B*, 2001, **105**, 4531.
25 E. Garrone, B. Bonelli, A. A. Tsyganenko, M. Rodríguez Delgado, G. Turnes Palomino, O. V. Manoilova and C. Otero Areán, *J. Phys. Chem. B*, 2003, **107**, 2537.
26 V. Bolis, B. Fubini, E. Garrone, E. Giamello and C. Morterra, *Stud. Surf. Sci. Catal.*, 1989, **48**, 159.
27 V. Bolis, G. Magnacca and C. Morterra, *Res. Chem. Intermed.*, 1999, **25**, 25.
28 E. Garrone, B. Fubini, B. Bonelli, B. Onida and C. Otero Areán, *Phys. Chem. Chem. Phys.*, 1999, **1**, 513.
29 C. Otero Areán, A. A. Tsyganenko, E. Escalona Platero, E. Garrone and A. Zecchina, *Angew. Chem. Int. Ed.*, 1998, **37**, 3161.
30 P. Ugliengo, E. Garrone, A. M. Ferrari, A. Zecchina and C. Otero Areán, *J. Phys. Chem. B*, 1999, **103**, 4839.
31 C. Otero Areán, *Comments Inorg. Chem.*, 2000, **22**, 241.
32 K. I. Hadjiivanov and G. N. Vayssilov, *Adv. Catal.*, 2002, **47**, 307.
33 P. Yu. Storozhev, V. S. Yanko, A. A. Tsyganenko, G. Turnes Palomino, M. Rodríguez Delgado and C. Otero Areán, *Appl. Surf. Sci.*, 2004, **238**, 390.
34 A. M. Ferrari, K. M. Neyman and N. Rösch, *J. Phys. Chem. B*, 1997, **101**, 9292.
35 O. V. Manoilova, M. Peñarroya Mentruit, G. Turnes Palomino, A. A. Tsyganenko and C. Otero Areán, *Vib. Spectrosc.*, 2001, **26**, 107.
36 A. M. Ferrari, P. Ugliengo and E. Garrone, *J. Chem. Phys.*, 1996, **105**, 4129.
37 C. Otero Areán, A. A. Tsyganenko, O. V. Manoilova, G. Turnes Palomino, M. Peñarroya Mentruit and E. Garrone, *Chem. Commun.*, 2001, 455.
38 A. Zecchina, S. Bordiga, J. G. Vitillo, G. Ricchiardi, C. Lamberti, G. Spoto, M. Bjorgen and K. P. Lillerud, *J. Am. Chem. Soc.*, 2005, **127**, 6361.
39 I. S. Ignatyev and T. Sundius, *Chem. Phys. Lett.*, 2005, **406**, 273.
40 A. A. Tsyganenko, P. Yu. Storozhev and C. Otero Areán, *Kinet. Catal.*, 2004, **45**, 530.
41 A. Zecchina, C. Otero Areán, G. Turnes Palomino, F. Geobaldo, C. Lamberti, G. Spoto and S. Bordiga, *Phys. Chem. Chem. Phys.*, 1999, **1**, 1649.
42 B. Fubini, V. Bolis, A. Cavenago, E. Garrone and P. Ugliengo, *Langmuir*, 1999, **9**, 2712.
43 F. Di Renzo, B. Chiche, F. Fajula, S. Viale and E. Garrone, *Stud. Surf. Sci. Catal.*, 1996, **101**, 851.